

A 3-GHz Profiler for Precipitating Cloud Studies

WARNER L. ECKLUND, CHRISTOPHER R. WILLIAMS, AND PAUL E. JOHNSTON

Cooperative Institute for Research in Environmental Sciences, University of Colorado, Boulder, Colorado

KENNETH S. GAGE

National Oceanic and Atmospheric Administration, Aeronomy Laboratory, Boulder, Colorado

(Manuscript received 11 January 1998, in final form 22 May 1998)

ABSTRACT

A 3-GHz profiler has been developed by the National Oceanic and Atmospheric Administration's Aeronomy Laboratory to observe the evolution and vertical structure of precipitating cloud systems. The profiler is very portable, robust, and relatively inexpensive, so that continuous, unattended observations of overhead precipitation can be obtained, even at remote locations. The new profiler is a vertically looking Doppler radar that operates at S band, a commonly used band for scanning weather radars (e.g., WSR-88D). The profiler has many features in common with the 915-MHz profiler developed at the Aeronomy Laboratory during the past decade primarily for measurement of lower-tropospheric winds in the Tropics. This paper presents a description of the new profiler and evaluates it in the field in Illinois and Australia in comparison with UHF lower-tropospheric profilers. In Illinois, the new profiler was evaluated alongside a collocated 915-MHz profiler at the Flatland Atmospheric Observatory. In Australia it was evaluated alongside a 920-MHz profiler during the Maritime Continent Thunderstorm Experiment. The results from these campaigns confirm the approximate 20-dB improvement in sensitivity, as expected for Rayleigh scatter. The results show that the new profiler provides a substantial improvement in the ability to observe deep cloud systems in comparison with the 915-MHz profilers.

1. Introduction

It is widely recognized that one of the greatest challenges in the numerical simulation of the atmosphere is the realistic simulation of the hydrological cycle. The simulation of clouds and precipitation in numerical models is still rudimentary. Clouds of all kinds have radiative impacts that are important for the heat budget of the atmosphere, and precipitation in cloud systems is the source of most diabatic heating that drives the Hadley and Walker circulations. Since atmospheric circulation is sensitive to the distribution of the diabatic heating (e.g., Hartmann et al. 1984), the specification of realistic distributions of diabatic heating is probably the greatest unmet need in numerical models of the atmosphere. To improve the parameterization of atmospheric heating due to the release of latent heat in precipitating cloud systems, it is necessary to develop global climatologies of the structure of precipitating cloud systems (Johnson 1984; Houze 1989). Although satellites provide useful information on the horizontal distributions of cloud imagery, they do not give detailed

information on vertical structure. It is important, therefore, to determine climatologies of the vertical structure of cloud systems especially in the Tropics. Several major international programs are addressing this need. Among them are the Global Energy and Water Cycle Experiment (GEWEX), designed to improve the understanding of the hydrological cycle, and the Global Ocean Atmosphere Land Surface (GOALS) program, designed to improve numerical modeling and prediction of the atmosphere-ocean-land surface system on a regional to global scale. Other programs such as the Tropical Rainfall Measuring Mission (TRMM) and the Atmospheric Radiation Measurement (ARM) are also directly concerned with this problem.

During the past decade, wind profiling radars have become an accepted tool for meteorological research and for operational applications. The wind profilers usually operate at longer wavelengths than conventional weather radars, and, at least in the clear atmosphere, the dominant scattering mechanism is Bragg scattering from refractive index inhomogeneities created by turbulence (e.g., Balsley and Gage 1982; Gage 1990). However, the 400-MHz National Oceanic and Atmospheric Administration (NOAA) demonstration network profilers and the 1-GHz lower-tropospheric wind profilers are quite sensitive to hydrometeors, insects, and birds (Ralph 1995; Wilczak et al. 1995).

Corresponding author address: Warner L. Ecklund, NOAA, ERL, Aeronomy Laboratory, 325 Broadway R/E/AL3, Boulder, CO 80303.
E-mail: wle@al.noaa.gov

Although wind profiling has been the major capability of profilers used in field campaigns and routine operations to date, there has been an increasing recognition of the utility of profilers for precipitation research (e.g., Wakasugi et al. 1985; Wakasugi et al. 1987; Gossard 1988; Gossard et al. 1990; Gossard et al. 1992; Rogers et al. 1993a,b; Ralph 1995; Gage et al. 1996). The profilers provide a vertically looking continuous view of the evolution of precipitating cloud systems that can be used in a manner foreseen in the work of Atlas et al. (1973). The profilers can be used to study rain over a substantial height range (Gage et al. 1994; Gage et al. 1996; Ecklund et al. 1995; Williams et al. 1995) due to the relatively high height of the melting layer in the Tropics. The profilers provide a continuous height-resolved measurement of reflectivity from a few hundred meters above the surface. The need for this capability as a complement to conventional scanning radar observations was pointed out in an excellent review by Joss and Waldvogel (1990).

During the late 1980s and early 1990s, the NOAA Aeronomy Laboratory developed the boundary layer wind profiler primarily for the measurement of lower-tropospheric winds in the deep Tropics (Ecklund et al. 1988; Ecklund et al. 1990; Carter et al. 1995). This profiler is very reliable and quite portable, and was an important component of the Tropical Oceans Global Atmosphere Coupled Ocean-Atmosphere Response Experiment (TOGA COARE) Integrated Sounding System (Parsons et al. 1994). As pointed out by Gage et al. (1994, 1996), the 915-MHz profiler is a unique tool for diagnosing precipitating cloud systems. The observations are recorded essentially continuously, so that a vertically directed profiler can observe with high vertical resolution the evolution of precipitating cloud systems above the profiler. This capability was employed for the first time during COARE and the COARE profiler observations contain a wealth of information about the structure and temporal variability of convective storms in the Tropics.

Observations at Manus Island, Papua New Guinea, in TOGA COARE with the 915-MHz profiler showed that hydrometeors were present in deep clouds above 5 km approximately 25% of the time. However, the 915-MHz profiler has limited sensitivity to high clouds. The 3-GHz profiler was developed in order to extend the height coverage of the profiler observations of these deep cloud systems. Deep cloud systems in the Tropics are thought to play a very important role in the global heat budget (e.g., Ackerman et al. 1988; Lubin et al. 1996). The frequency of 3 GHz was selected because it provided a substantial gain in sensitivity without encountering significant rain attenuation, which is a known problem for cloud radars operating near 33 and 94 GHz.

In the past decade, substantial progress has been made in the development of cloud radars capable of monitoring cloud systems with high temporal and spatial resolution (e.g., Lhermitte 1987; Sassen 1987; Matrosov

1992; Clothiaux et al. 1995; Sekelsky and McIntosh 1996). The 3-GHz profiler has been operated with low temporal and spatial resolution compared to most cloud radars in order to improve sensitivity. This means that observed cloud edges and cloud thicknesses have not been as well resolved as would be possible with typical millimeter wavelength cloud radars. However, the 3-GHz profiler can monitor much of the important precipitating cloud structure and has the advantage of not being affected by attenuation. The examples that are contained in this paper are drawn from observations made at both midlatitude and tropical sites. The Flatland Atmospheric Observatory (FAO) is located in Bondville, Illinois, near the University of Illinois in Urbana, and Garden Point is located on Melville Island off the coast of Australia near Darwin. In both cases the 3-GHz (2835 MHz) profiler was collocated with a 1-GHz (915 MHz, 920 MHz) profiler. The measurements confirm an approximate 20-dB improvement in sensitivity of the 3-GHz profiler over the sensitivity of the 1-GHz profiler due to the wavelength dependence of Rayleigh scattering. This improvement is sufficient to enable the observation of cloud tops to tropopause altitudes. At times, when rain is not falling to the surface, the observations reveal extensive shields of optically thick clouds.

In this paper, we stress the improved sensitivity of the new 3-GHz profiler for observation of precipitating clouds. Section 2 contains a description of the new profiler, and section 3 contains observations taken with the new profiler at FAO and in Australia during the Maritime Continent Thunderstorm Experiment (MCTEX). The observations are discussed in section 4, and our conclusions are stated in section 5.

2. 3-GHz profiler description

The 3-GHz radar described in this paper is a relatively simple and inexpensive vertically pointing Doppler radar that uses profiler technology. The profiler is quite portable, so that it can be installed quickly in remote locations, if desired. It operates unattended with low operating and maintenance costs and provides high-resolution profiles of the vertical structure of overhead cloud systems with nominal 30-s time resolution. The continuous vertical observations provided by the profiler are complementary to observations from scanning Doppler radars that nominally spend about 5 min per volume scan. The simple profiler provides a continuous overhead view of clouds with good time resolution, while the scanning radar provides a description of the scanned volume with lower time resolution and with poorer vertical resolution with increasing range.

The 3-GHz profiler uses much of the same hardware and software used in our 1-GHz (915 and 920 MHz) profilers described in Carter et al. (1995) with the exception of the transmitter and antenna. The operating frequency for this profiler was chosen based on our desire to have the best sensitivity to precipitation and



FIG. 1. The 3-GHz profiler dish antenna and shroud as configured for FAO and MCTEX.

still be able to use a reliable, safe, and relatively inexpensive solid-state transmitter. The nominal 350-W peak-power transmitter module is described in Hanczor and Kumar (1993). The transmitter is located in the transmit–receive (T/R) module mounted on the edge of the shrouded dish antenna in a protective housing. Figure 1 shows the housing and the antenna feed suspended at the focal point of the parabolic reflector by four fiberglass spars. This arrangement minimizes the length and loss of the feed cable between the T/R module and the antenna feed, and mounts the T/R module at a convenient working height.

The antenna is fixed to point in the vertical direction. The perimeter shroud reduces the unwanted effects of feed spillover and ground clutter. The dish is underilluminated so that the beamwidth is 3.2° with a first sidelobe level about 25 dB below the main beam. The antenna beamwidth and sidelobe levels have been verified by solar scans in the Tropics (A. Riddle 1997, personal communication). The far sidelobes at low elevation have not been measured; however, we observe that ground clutter seems to be reduced compared with our experience with other profilers. The T/R module located at the antenna communicates with transmit and

TABLE 1. Typical parameters used at Garden Point, Australia, during MCTEX.

Parameters	3-GHz profiler	1-GHz profiler
Frequency (MHz)	2835	920
Wavelength (cm)	10.6	32.6
Peak power (W)	380	500
Antenna	3-m shrouded dish	2-m phased array
Beamwidth (deg)	3.2	9
Height resolution (m)	100 and 500	100 and 500
Maximum height sampled (km)	21.4	21.4
Coherent integrations	8	25
Maximum radial velocity (m s^{-1})	± 20	± 20
Spectral points	128	128
Dwell time (s)	35	35
Recording	Full spectra	Full spectra

receive units inside a nearby shelter via 60-MHz signals carried on two coaxial cables. The received phase-coherent signal is converted to baseband and the resulting quadrature channels are filtered, amplified, and range sampled with 8-bit digitizers. The resulting time series at each sampled range gate are further time averaged and then processed to produce 128-point Doppler power spectra at each sampled height, as described in Carter et al. (1995). During typical 30-s dwell times at each sampled height, about 120 spectra are produced at 3 GHz, and these are averaged together and recorded on optical or magnetic media.

Typical parameters for the 3- and the 1-GHz profiler to which it is compared in this paper are given in Table 1. Note that the 1-GHz antenna beamwidth is nearly three times the beamwidth of the 3-GHz profiler. Much of our work is in the Tropics, where the tropopause and deep convective activity may extend to altitudes of more than 18 km. In this environment, we set the profiler interpulse period so that heights of up to about 22 km are not range aliased. We also set the maximum unaliased Doppler velocity to about plus or minus 20 m s^{-1} in order to capture the large up- and downdrafts often present in deep convection. To date, we have used primarily 500-m vertical resolution since we wanted to detect the presence of deep precipitating clouds with good sensitivity. Typically, we record a sequence of nine 30-s average spectra with 500-m resolution, and one 30-s average spectrum with 100-m resolution. Typical minimum and maximum sensitivities for both profilers in dBZ_e versus height are shown in Fig. 2. These values are calculated for 500-m height resolution using known system parameters and 30-s dwell times. The dynamic range of each profiler is limited to about 50 dB by the 8-bit digitizers. The crosshatched area in Fig. 2 shows the range of reflectivities over which the two profilers can be intercompared as a function of height.

3. Observations from 3-GHz profilers

The first test of the prototype 3-GHz profiler was conducted at the FAO. The Flatland site was selected

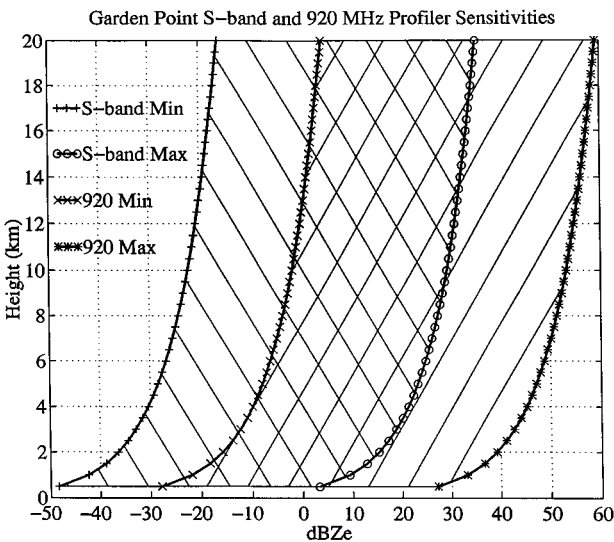


FIG. 2. Detection and saturation thresholds for the 3- and 1-GHz profilers operated in the high mode (500-m resolution).

because of its location on flat terrain and the 50- and 915-MHz profilers that are maintained at Flatland by the Aeronomy Laboratory. The Flatland experiments included a substantial period of simultaneous observation of the 3-GHz profiler with the collocated 915-MHz profiler. The Flatland 915-MHz profiler has a nine-panel antenna that is larger than the standard 915-MHz profiler antenna used at the Aeronomy Laboratory tropical profiler sites. The intercomparison of observations from the two profilers during this prolonged campaign yielded a wealth of new information concerning the nature of the echoes being observed. As pointed out by Wilson et al. (1994), the echoes observed by weather radars at comparable wavelengths are often contaminated by insects, birds, or hydrometeors.

The use of two profilers observing the same volume of the atmosphere permits the unambiguous determination of the type of scattering being observed. For example, Knight and Miller (1993) have examined “mantle echoes” in the early stages of precipitation from clouds and found that they are due to Bragg scattering. Recently, Rogers and Brown (1997) have used Doppler radar operating at several frequencies to investigate backscattering from a smoke plume that lofted over McGill University in Montreal, Quebec, Canada. The use of differential reflectivity to diagnose the nature of backscattering from collocated profilers in the Tropics is presented by Gage et al. (1999, manuscript submitted to *J. Atmos. Sci.*).

a. The Flatland observations

An example of 3-GHz profiler observations of high-altitude clouds over central Illinois in advance of an extratropical disturbance in October 1994 is shown in Fig. 3. The time–height section in Fig. 3 shows the

appearance of a deep cloud system just below 11 km after 0000 LT 15 October 1994. While the top of the cloud system is maintained at an altitude close to 11 km, the bottom of the cloud system progressively decreases in altitude from about 10 km at 0000 LT down to 3 km at 1700 LT on 15 October. At 0600 UTC, a closed low was located over southern Utah. Ahead of this, a deep circulation southerly flow extended as far north and as far east as Ohio. This circulation remained nearly stationary during the next 24 h. The deep cloud system evidenced by the radar reflectivity shown in the top panel of Fig. 3 is associated with the “warm conveyor belt” (e.g., Cotton and Anthes 1989), with upward vertical motion (often referred to as “slantwise convection”) accompanying the deep southerly flow on the eastward flank of the upper-level disturbance.

The middle panel of Fig. 3 shows the Doppler velocity recorded by the profiler. The Doppler velocities are mostly in the range of a few tens of centimeters per second to 2 m s^{-1} downward. Around 0000 LT, the Doppler velocities are quite small and are associated with thick cirrus. As the clouds thicken and lower, the Doppler velocities increase with the largest Doppler velocities at the lower portion of the clouds where they increase to $2\text{--}3 \text{ m s}^{-1}$ by 1100 LT.

The clouds in Fig. 3 are composed of frozen hydrometeors, and their fall velocities are consistent with fall velocities of frozen precipitation. None of the precipitation in Fig. 3 reaches the lower troposphere, and certainly not the surface, implying that the falling hydrometeors evaporate beneath the clouds. The evaporation of the falling hydrometeors beneath the clouds acts to cool and moisten the middle troposphere.

Another feature worth noting in Fig. 3 is the mesoscale structure in the evolution of reflectivities and Doppler velocities. There appears to be a modulation of the structure of the echoes with a period of order 1 h. These fluctuations are likely associated with gravity waves that are commonly associated with disturbed weather.

b. The Garden Point, Australia, observations

During the MCTEX field campaign, a 920- and a 2835-MHz profiler were collocated at Garden Point on Melville Island about 100 km northwest of Darwin, Australia, as shown on the map in Fig. 4. The purpose of MCTEX was to study the life cycle of convective storms over Melville and Bathurst Islands. These Tiwi Islands provide an ideal natural laboratory for studying tropical convection because deep convective systems regularly develop over the islands on a daily basis during the rainy season owing to the organization of boundary layer convergence by the prevailing sea-breeze circulation (Keenan et al. 1996).

Two examples of deep convective cloud systems observed by the Garden Point profilers are presented here. The first example is of a squall line that passed over Garden Point in the early afternoon of 28 November

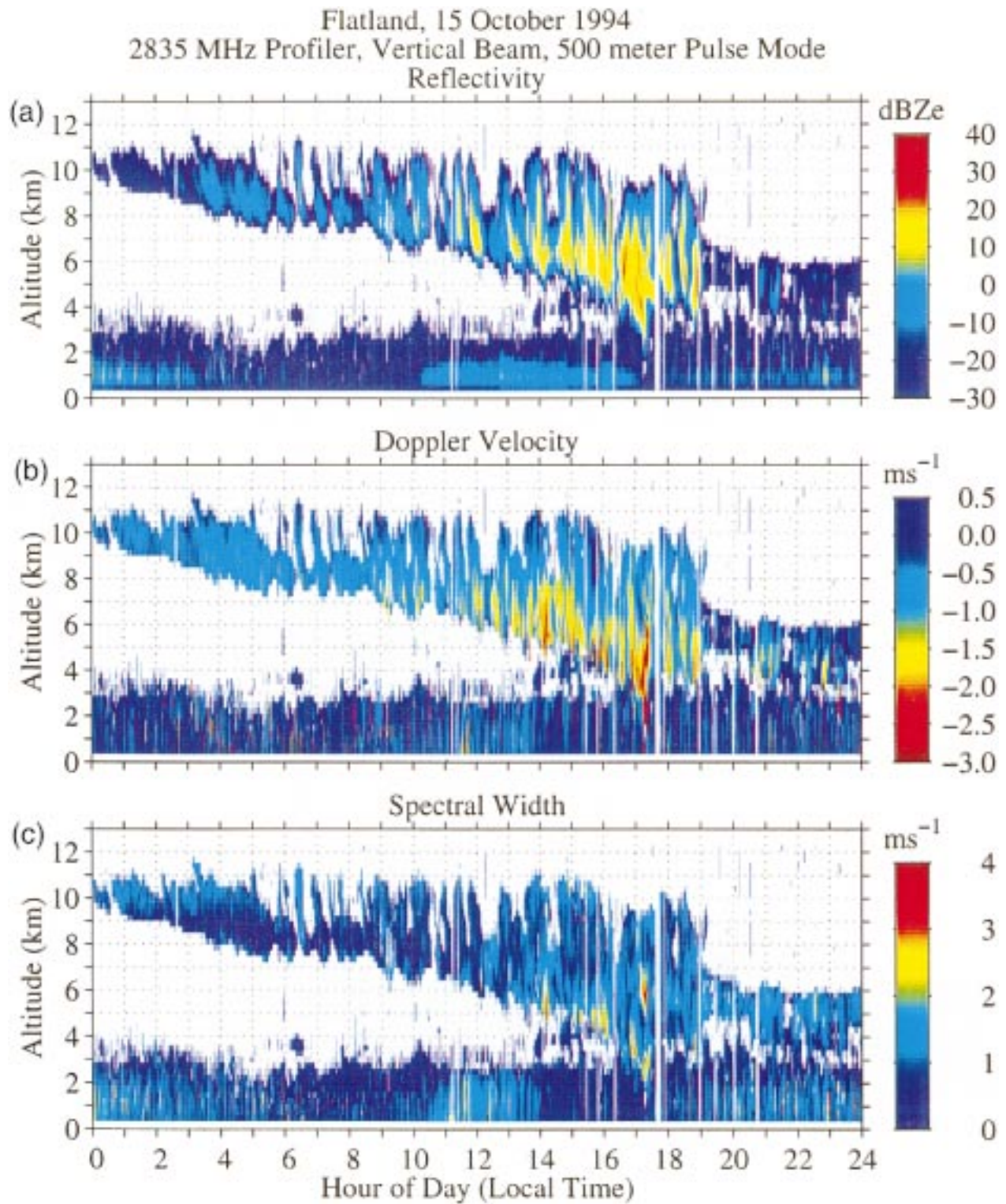


FIG. 3. Time–height sections of (a) equivalent reflectivity, (b) Doppler velocity, and (c) spectral width for observations made by the 3-GHz profiler at the Flatland Atmospheric Observatory on 15 October 1994.

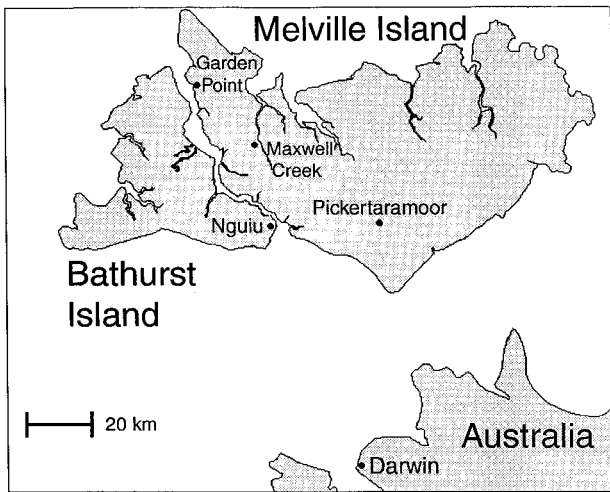


FIG. 4. Map of the Tiwi Islands in Australia, which was the site of the MCTEX field campaign.

1995. The second example is of a deep convective anvil structure over Garden Point during the afternoon of 3 December 1995. On this second day, the initial deep convection missed Garden Point so that the hydrometeors observed over Garden Point were lofted into the upper troposphere by deep convection located some distance from Garden Point.

The first example of deep convection observed during MCTEX by the 3-GHz profiler is presented in Fig. 5. The equivalent reflectivity, Doppler velocity, and spectral width observed on 28 November at Garden Point by the 3-GHz profiler are contained in Fig. 5. The convective echo reaches its highest altitude of 18 km at 1330 LT, and within about 2 h decreases overhead to about 14 km. From 1500 until 1900 LT, the top of the anvil structure gradually decreases to about 11 km. Consider first the evolution of the reflectivity structure above 5 km. After an initial burst of reflectivity up to about 30 dBZ_e reaching an altitude of over 18 km, the highest reflectivity values recede within about an hour to below 11 km. A broad band of equivalent reflectivity of less than 10 dBZ_e extends above about 10 km, and gradually, the top of the 10-dBZ_e contour decreases in altitude until it disappears at 8 km at about 1700 LT. At the melting level and below, the equivalent reflectivities of the 3-GHz profiler are limited by saturation to values less than about 20 dBZ_e. The highest values of equivalent reflectivity around the melting level occur at the beginning of the convective storm and persist for several hours. However, the longest persisting layer of hydrometeors is located at about 11 km. Note also the region of large reflectivities beginning about 1830 LT at 1–3 km. These strong echoes are most likely due to bats or other nighttime flyers.

Doppler velocity and spectral width observed by the 3-GHz profiler are contained in the middle and bottom panels of Fig. 5. The Doppler velocity shows large fall

velocities in the active early stages of the convective storm. As the most active convection subsides after 1400 LT, there is evidence of a quasi-periodic, nearly vertically aligned modulation of the deep anvil structure above 5 km. At the melting level, the acceleration of melting hydrometeors is clearly visible and Doppler velocities are in the range of -6 to -8 m s⁻¹. Before 1330 LT and after 1700 LT, the lower-tropospheric echoes are primarily due to Bragg scatter and have Doppler velocities in the range of ± 1 m s⁻¹ (except for the strong echoes commencing at about 1830 LT). The spectral width is very large in the early stages of convection between 1300 and 1400 LT. Spectral width decreases gradually after 1400 LT. Note also the enhanced values of spectral width that accompany the enhanced values of reflectivity at 1–2 km beginning at about 1830 LT.

Equivalent reflectivity, Doppler velocity, and spectral width seen by the collocated 920-MHz profiler on 28 November are shown in Fig. 6. The equivalent reflectivity in the top panel shows approximately the same structure as can be seen in the top panel of Fig. 5 except that the 920-MHz profiler does not observe the weaker echoes near the top of the anvil structure. Note that the 920-MHz profiler is less affected by saturation of the strongest echoes near and below the melting level. The magnitude of this systematic reduction in sensitivity to hydrometeors is consistent with the approximate 20-dB difference expected in sensitivity for Rayleigh scattering at the two profiler frequencies of 2835 and 920 MHz. However, at the lower levels where Bragg scattering from refractivity turbulence is dominant, the 920-MHz profiler exhibits increased reflectivity when expressed in terms of dBZ_e.

Doppler velocity and spectral width for the 920-MHz observations are shown in the middle and bottom panels of Fig. 6. In both cases, the Doppler velocity and spectral width are very similar to what is seen in Fig. 5 for the 3-GHz profiler even though the 920-MHz profiler beamwidth is nearly three times wider than the beamwidth of the 3-GHz profiler.

A second example of deep convection observed during MCTEX by the two profilers is shown in Figs. 7 and 8. Figure 7 contains the 3-GHz observations of an elevated anvil structure observed over Garden Point during 3 December 1995. In this example, only hydrometeors are observed above about 5 km, and this structure is undoubtedly composed exclusively of frozen hydrometeors. Since there are no hydrometeors present below about 6 km, the profilers are not saturated as they were on 28 November. In this example, the anvil structure persists for about 6 h, with maximum reflectivities of about 20 dBZ_e in the 6–12-km range. Just after 1430 LT, when the tropospheric anvil is first observed, it extends up to about 17 km, which is close to the height of the tropical tropopause at this time of year. The top of the structure gradually descends with time until it reaches about 13 km at about 1930 LT. The bottom of the structure is maintained near 6 km for about 4 h until

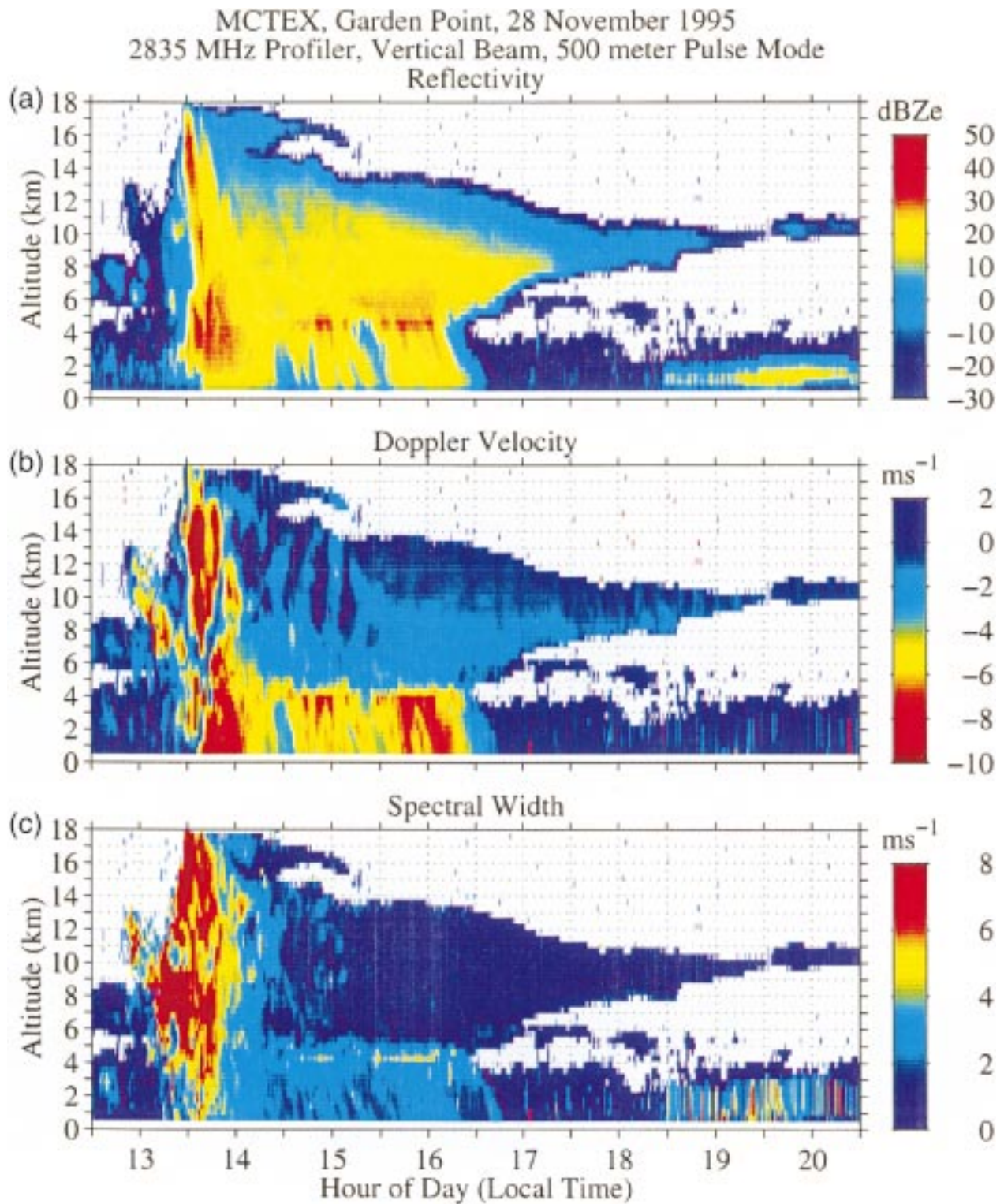


FIG. 5. Time-height sections of (a) equivalent reflectivity, (b) Doppler velocity, and (c) spectral width for observations made by the 3-GHz profiler at Garden Point on 28 November 1995.

MCTEX, Garden Point, 28 November 1995
920 MHz Profiler, Vertical Beam, 500 meter Pulse Mode
Reflectivity

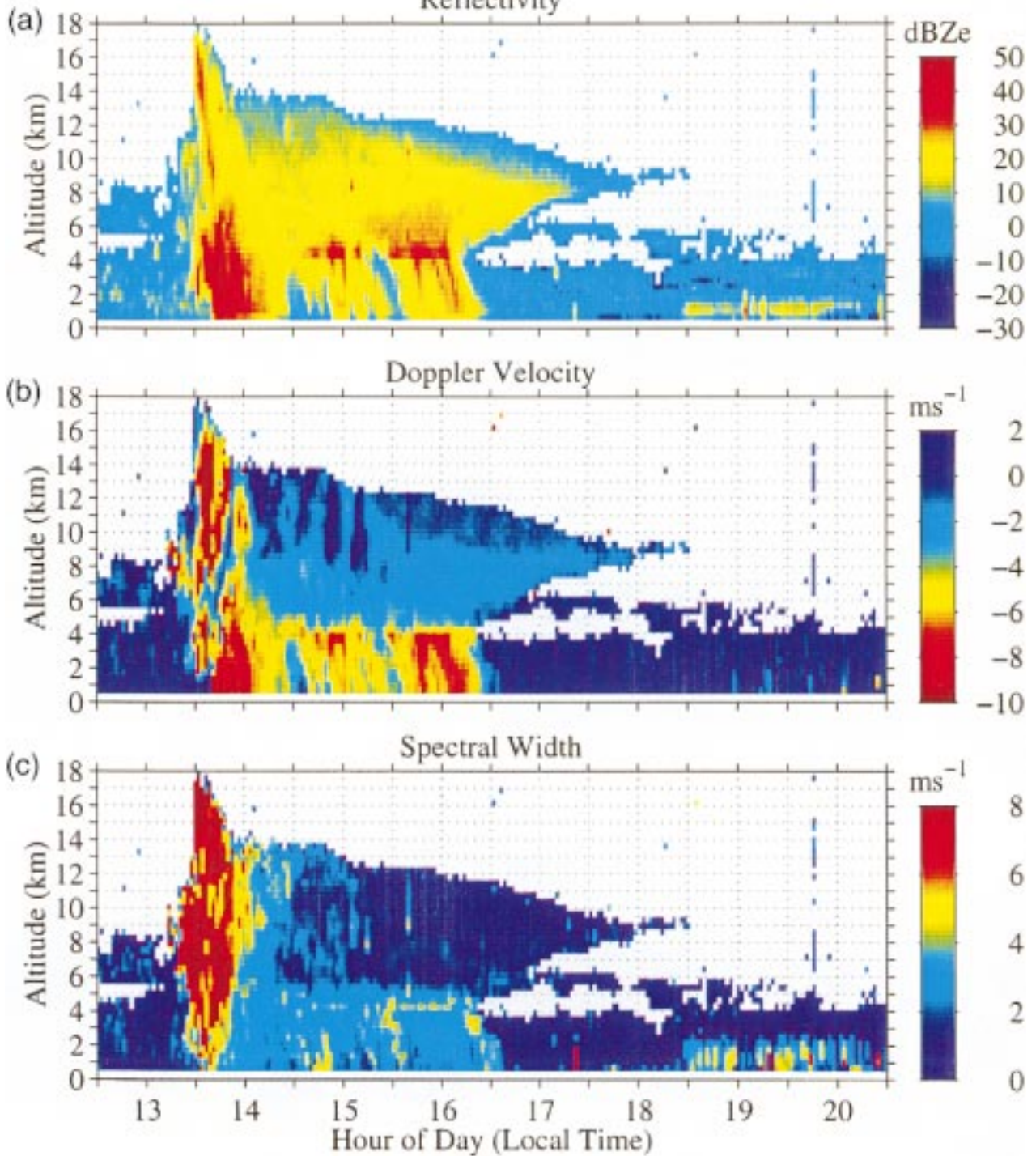


FIG. 6. Time–height sections of (a) equivalent reflectivity, (b) Doppler velocity, and (c) spectral width for observations made by the 920-MHz profiler at Garden Point on 28 November 1995.

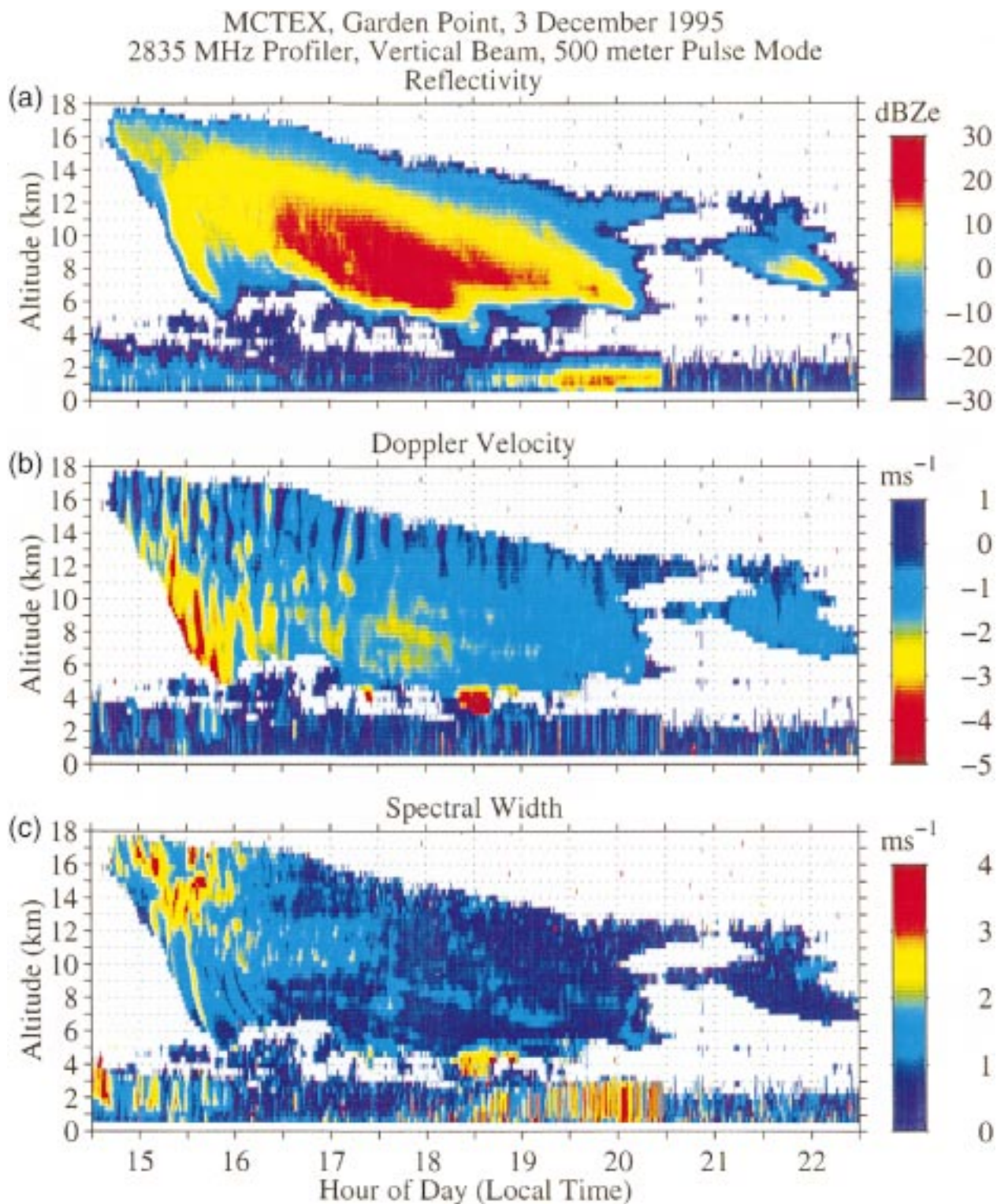


FIG. 7. Time-height sections of (a) equivalent reflectivity, (b) Doppler velocity, and (c) spectral width for observations made by the 3-GHz profiler at Garden Point on 3 December 1995.

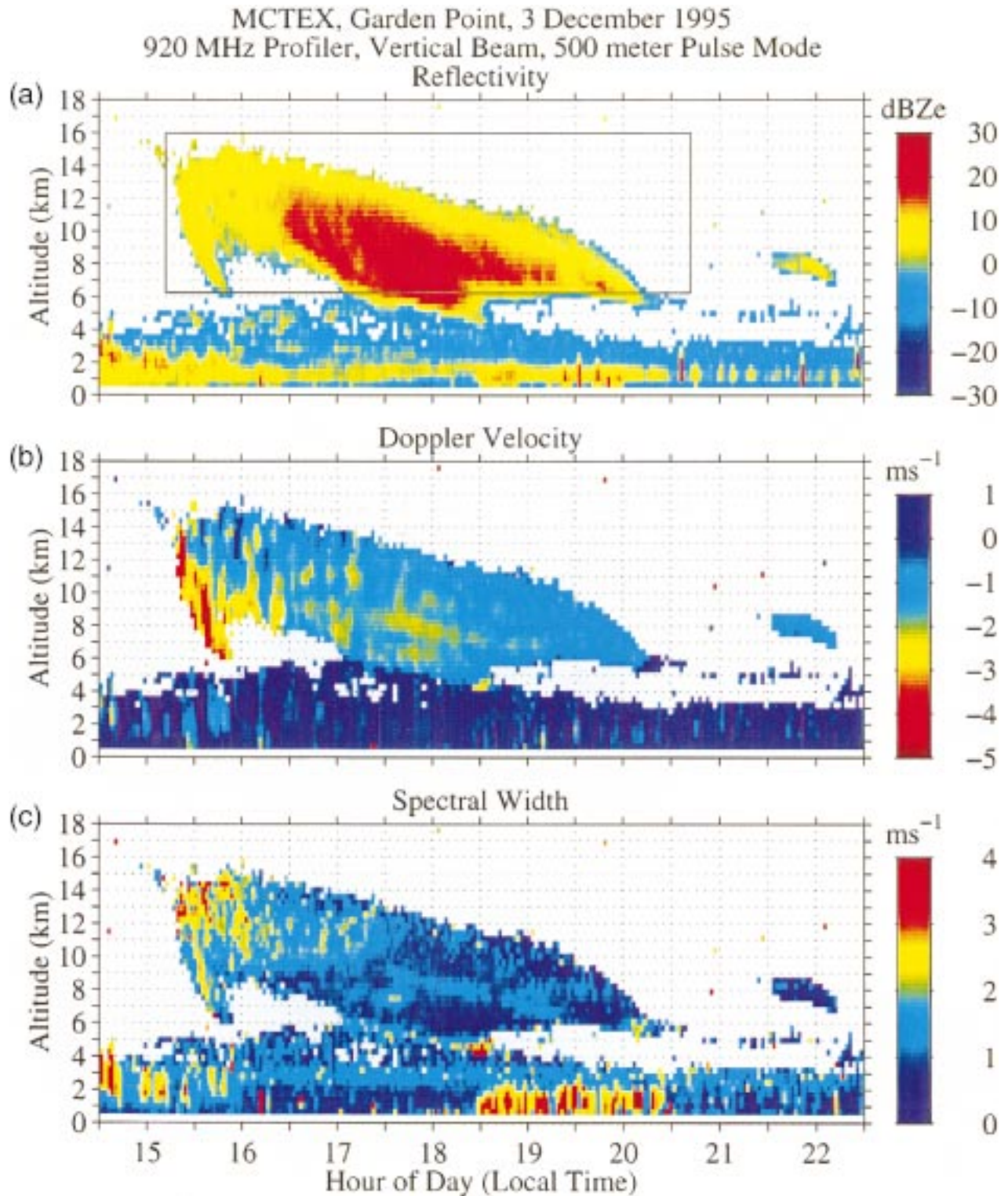


FIG. 8. Time–height sections of (a) equivalent reflectivity, (b) Doppler velocity, and (c) spectral width for observations made by the 920-MHz profiler at Garden Point on 3 December 1995. The box in (a) defines the domain in which the scatterplot in Fig. 9 is constructed.

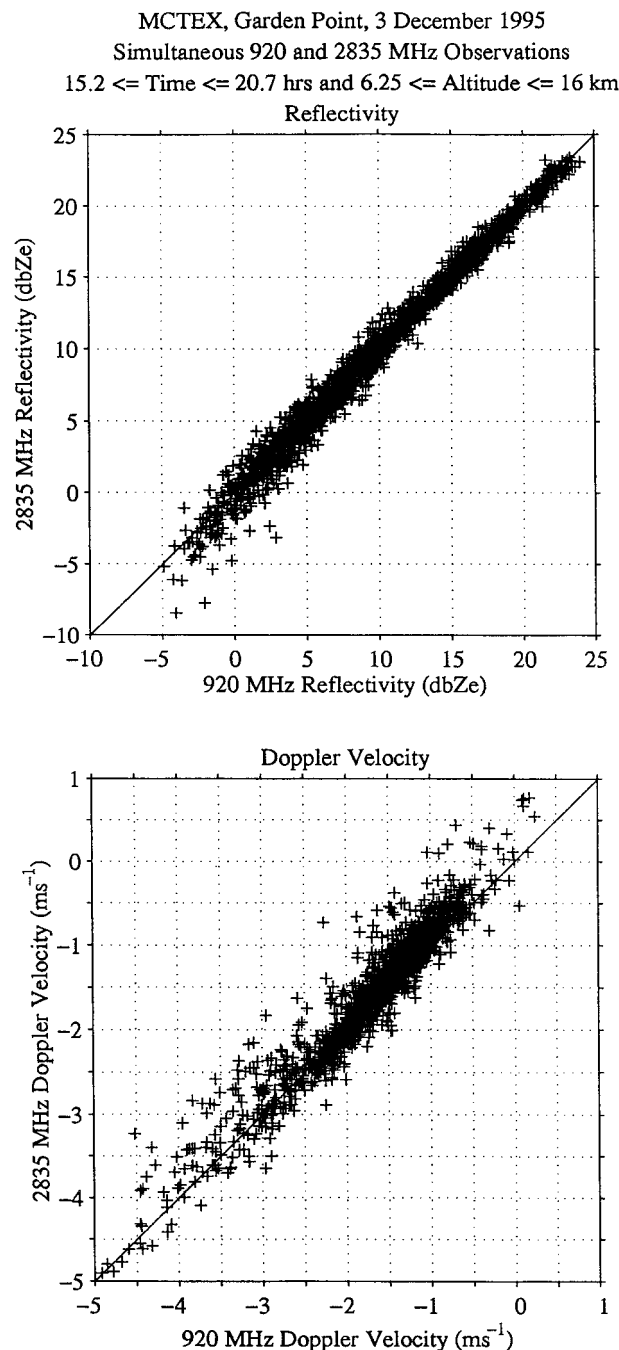


FIG. 9. Scatterplot of (a) equivalent reflectivity and (b) Doppler velocity observed by 3-GHz and 920-MHz profilers within the box shown in Fig. 8a.

2000 LT. The top of the region of equivalent reflectivity in excess of 20 dBZ_e decreases on average about 2 km per hour. The time rate of descent of the bottom of this region of strongest equivalent reflectivity is somewhat larger. On 3 December there also appear to be enhanced echoes below 3 km beginning at about 1830 LT, which is consistent with echoes from nighttime flyers.

Doppler velocities observed by the 3-GHz profiler are shown for the same period in the middle panel of Fig. 7. Fall velocities are reflectivity weighted to the larger particles that have the greatest fall velocity. Nevertheless, in the top half of the anvil, the Doppler velocities range is ± 1 m s⁻¹. Note the vertically oriented banded structure indicative of gravity wave activity that seems to be most pronounced in the upper part of the anvil. Similar structures have been simulated in numerical models of mesoscale convective systems (e.g., Alexander et al. 1995).

The corresponding observations from the collocated 920-MHz profiler are contained in Fig. 8. In this example, the 920-MHz profiler observes only equivalent reflectivities exceeding about 0 dBZ_e above 6 km, while the 3-GHz profiler is sensitive down to about -20 dBZ_e, as diagrammed in Fig. 2. Note in Figs. 7 and 8 the increase in equivalent reflectivity and spectral width variance below about 2 km after 1830 LT, showing evidence of scattering from discrete targets such as bats, birds, or insects.

The Rayleigh scattering observations from the 1- and 3-GHz profilers are compared by constructing scatterplots of the observations that are within 60 s of each other and at the same range-gate distance. The equivalent reflectivity and Doppler velocity above 6.25 km, where Rayleigh scatter from hydrometeors is the dominant scattering process, are shown in Fig. 9. The box in Fig. 8a outlines the time-height domain from 1512 to 2042 LT and 6.25–16 km for data used in Fig. 9. There is excellent agreement between the equivalent reflectivities and Doppler velocities during these Rayleigh scattering observations.

In the lower troposphere, where both Rayleigh and Bragg scattering occur, the difference of about 18 dB in equivalent reflectivities shown in Figs. 7 and 8 results from the different sensitivities to Bragg scattering at 1 and 3 GHz. Briefly, in the absence of Rayleigh scatterers, the profilers obtain backscattering from the refractive index irregularities created from atmospheric turbulence acting upon refractive index gradients. This kind of scattering, commonly referred to as Bragg scattering, is only weakly dependent on the radar wavelength, provided the radar half-wavelength lies within the inertial subrange of homogeneous, isotropic turbulence. Usually, Bragg scattering is quantified in terms of C_n^2 , the refractivity turbulence structure constant. When expressed in terms of equivalent reflectivity, the reflectivity difference is close to 18 dB for Bragg scattering observed by profilers operating at 1 GHz and 3 GHz, provided the half-wavelength of the two profilers lies within the inertial subrange. Differential reflectivities using profilers at these frequencies can be used to unambiguously identify the type of echo being observed (Gage et al. 1999).

4. Discussion

The experience with the new 3-GHz profiler both in Illinois and Australia has been to substantially extend

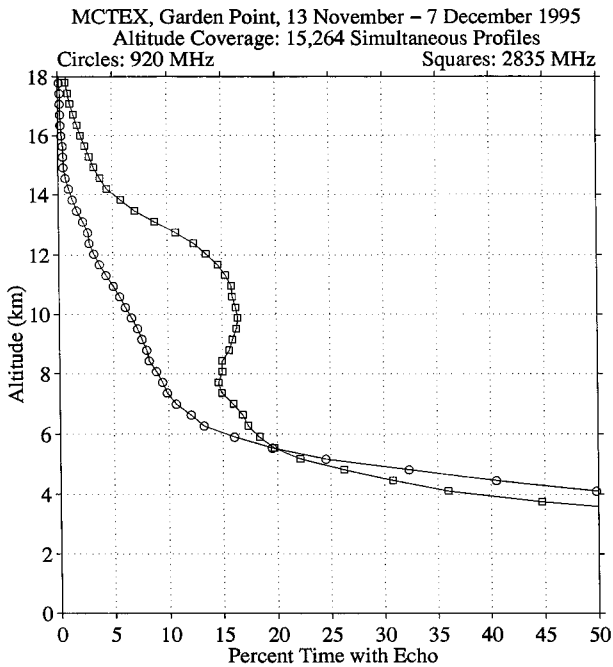


FIG. 10. Altitude coverage for the 920- and 2835-MHz profilers in Australia during the MCTEX field campaign, November–December 1995.

the height coverage of 1-GHz profiler observations of precipitating cloud structures. At 10 km the sensitivity of the 3-GHz profiler in the 500-m height-resolution mode is -22 dBZ_e, which is about 20 dB more sensitive than the 1-GHz profiler in its 500-m height mode. Most of this 20-dB difference in sensitivity is attributable to the increased sensitivity of the higher-frequency 3-GHz profiler to Rayleigh scattering when hydrometeors are present. A comparison of the equivalent reflectivities observed for 28 November (Figs. 5 and 6) and for 3 December (Figs. 7 and 8) show clearly the increased sensitivity of the 3-GHz profiler.

Statistics of the height coverage for the 3-GHz and 915-MHz profilers used in MCTEX in Australia are shown in Fig. 10. At the lowest levels (i.e., below 5 km), the height coverage of the 920-MHz profiler exceeds the 3-GHz profiler because in this altitude range the observed echoes are primarily from the “clear air.” Above about 6 km the only echoes observed by both profilers are from hydrometeors. Since the 3-GHz profiler is about 20 dB more sensitive to Rayleigh scattering than the 920-MHz profiler, the 3-GHz profiler observes substantially more echoes than the 920-MHz profiler. For example, at 10 km there is a relative maximum of 17% in the percent of time that hydrometeors were observed at this altitude by the 3-GHz profiler in comparison to 7% of the time that hydrometeors were observed at 10 km by the 920-MHz profiler. Above 12 km, the percent time hydrometeors are observed by both profilers decreases rapidly with altitude. However, even at 14 km the 3-GHz profiler observes hydrometeors 5%

of the time compared with the roughly 1% of the time that hydrometeors can be observed at this altitude by the 920-MHz profiler. We attribute the large difference in occurrence observed by the two profilers around 10 km to the distribution of reflectivities in this height range. Reflectivity distributions in tropical precipitating clouds will be presented in a separate paper.

These results can be contrasted with what has been observed at Manus Island with the 915-MHz profiler, as reported by Gage et al. (1994) and Ecklund et al. (1995). These authors found that, at Manus Island, hydrometeors were observed above 5 km 20%–25% of the time. Thus, even with the enhanced capability to observe hydrometeors with the 2835-MHz profiler evidenced in Fig. 10, the hydrometeor occurrence above 5 km is lower at Garden Point than at Manus Island. Recent observations from Manus Island using the same 2835-MHz profiler that was used at Garden Point in MCTEX show that there is a substantially greater occurrence of hydrometeors at Manus Island. For example, the recent results for Manus Island in early 1996 show a hydrometeor occurrence at 10 km that is about 7% for the 915-MHz profiler and 27% for the 2835-MHz profiler increasing at lower altitudes to more than 35% at 5 km.

The 3-GHz profiler is well suited to observation of deep cloud systems in the Tropics and midlatitudes and can be used very effectively to monitor precipitating clouds above a given site. Moreover, it is also very useful in combination with a 1-GHz profiler as a research tool to unambiguously separate Rayleigh scattering from particulates and Bragg scattering from refractivity inhomogeneities associated with turbulence.

Other instruments were deployed to observe clouds at Garden Point during MCTEX. The University of Massachusetts had 35- and 94-GHz cloud radars collocated with the 1- and 3-GHz profilers. The observations from the cloud radars have been analyzed in combination with the 3-GHz observations to yield estimates of particle size distributions in deep cloud systems (Sekelsky et al. 1999). The three frequencies yield substantially better estimates of particle size distributions than can be obtained by the two cloud radars alone.

5. Conclusions

A prototype 3-GHz profiler has been constructed and tested in the field alongside a 915-MHz profiler in Illinois at the Flatland Atmospheric Observatory and alongside a 920-MHz profiler in Australia during MCTEX. The 3-GHz profiler provided a time history of the deep cloud systems at both sites. The profiler is well suited for long-term unattended height-resolved monitoring of cloud coverage. Since the 3-GHz profiler is about 20 dB more sensitive to hydrometeors than the 920-MHz profiler, it is better suited for precipitating cloud research than the 920-MHz profiler. The two profilers together provide a powerful research tool for un-

ambiguous identification of hydrometeors in profiler observations.

Our initial motivation for developing the 3-GHz profiler was to observe the precipitating clouds in the Tropics above 5 km with better sensitivity. To obtain good sensitivity, we have used a height resolution of 500 m and averaging time of about 30 s. Thus, the cloud edges and thicknesses presented here are not as well defined as they would have been by using millimeter-wavelength cloud radars. The observations presented here were obtained with 8-bit digitizers that have limited the dynamic range to about 50 dB. This limited range means that the 3-GHz profiler saturates at a reflectivity of about 18 dBZ_e at a height of 2 km, so that we have sacrificed quantitative observations of rain in the lower altitudes in favor of sensitivity to frozen hydrometeors at anvil altitudes. These preliminary observations suggest two different ways in which the 3-GHz profiler could be modified for future studies.

First, the sensitivity could be further increased to obtain sensitivities on the order of -35 dBZ_e at 10 km by using the full average power of the transmitter through pulse coding and also increasing the size of the antenna by a nominal amount. This would provide a reasonable way to monitor all but the most tenuous precipitating clouds on a continuous basis with a relatively modest profiler.

A second way the 3-GHz profiler can be exploited is to use the available 60- and 100-m height resolutions to obtain high-resolution vertical profiles of precipitation from near the surface to above the melting layer. The 100-m resolution profiles obtained in conjunction with the 500-m observations presented in this paper show detailed precipitation structure through the melting layer, including intense and thin bright bands. Since the 100-m resolution data yield quantitative reflectivities to within a few hundred meters of the ground, they are very useful in comparing profiler data with disdrometer and rain gauge data at the surface. The dynamic range of the 3-GHz profiler will be extended to near 75 dB by use of 12-bit digitizers in future studies. The 3-GHz profiler can also be modified for rain studies to extend the saturation level in heavy precipitation to more than 60 dBZ_e at a range of 1 km.

Acknowledgments. We thank W. L. Clark and J. M. Warnock for technical assistance in the Flatland experiment and the Australian Bureau of Meteorology Research Centre for technical assistance during the MCTEX field campaign. We also thank E. Clothiaux for his good-natured assistance with profiler operations during MCTEX. The research reported here was supported in part by the National Science Foundation under Grants ATM-9214800 and ATM-941638, the NOAA Office of Global Programs, and DOE ARM.

REFERENCES

- Ackerman, T. P., K. N. Liou, F. P. J. Valero, and L. Pfister, 1988: Heating rates in tropical anvils. *J. Atmos. Sci.*, **45**, 1606–1622.
- Alexander, M. J., J. R. Holton, and D. R. Durran, 1995: The gravity wave response above deep convection in a squall line simulation. *J. Atmos. Sci.*, **52**, 2212–2226.
- Atlas, D., R. C. Srivastava, and R. S. Sekhon, 1973: Doppler radar characteristics of precipitation at vertical incidence. *Rev. Geophys. Space Phys.*, **11**, 1–35.
- Balsley, B. B., and K. S. Gage, 1982: On the use of radars for operational wind profiling. *Bull. Amer. Meteor. Soc.*, **63**, 1009–1018.
- Carter, D. A., K. S. Gage, W. L. Ecklund, W. M. Angevine, P. E. Johnston, A. C. Riddle, J. S. Wilson, and C. R. Williams, 1995: Developments in UHF lower tropospheric wind profiling at NOAA's Aeronomy Laboratory. *Radio Sci.*, **30**, 977–1001.
- Clothiaux, E. E., M. A. Miller, B. A. Albrecht, T. P. Ackerman, J. Verlinde, D. M. Babb, R. M. Peters, and W. J. Syrett, 1995: An evaluation of a 94-GHz radar for remote sensing of cloud properties. *J. Atmos. Oceanic Technol.*, **12**, 201–229.
- Cotton, W. R., and R. A. Anthes, 1989: *Storm and Cloud Dynamics*. Academic Press, 880 pp.
- Ecklund, W. L., D. A. Carter, and B. B. Balsley, 1988: A UHF wind profiler for the boundary layer: Brief description and initial results. *J. Atmos. Oceanic Technol.*, **5**, 432–441.
- , —, —, P. E. Currier, J. L. Green, B. L. Weber, and K. S. Gage, 1990: Field tests of a lower tropospheric wind profiler. *Radio Sci.*, **25**, 899–906.
- , K. S. Gage, and C. R. Williams, 1995: Tropical precipitation studies using a 915-MHz wind profiler. *Radio Sci.*, **30**, 1055–1064.
- Gage, K. S., 1990: Radar observations of the free atmosphere: Structure and dynamics. *Radar in Meteorology*, D. Atlas, Ed., Amer. Meteor. Soc., 534–565.
- , C. R. Williams, and W. L. Ecklund, 1994: UHF wind profilers: A new tool for diagnosing tropical convective cloud systems. *Bull. Amer. Meteor. Soc.*, **75**, 2289–2294.
- , —, and —, 1996: Application of the 915-MHz profiler for diagnosing and classifying tropical precipitating cloud systems. *Meteor. Atmos. Phys.*, **59**, 141–151.
- Gossard, E. E., 1988: Measuring drop-size distributions in clouds with a clear-air-sensing Doppler radar. *J. Atmos. Oceanic Technol.*, **5**, 640–649.
- , R. G. Strauch, and R. R. Rogers, 1990: Evolution of droplet distribution in liquid precipitation observed by ground-based Doppler radar. *J. Atmos. Oceanic Technol.*, **7**, 815–828.
- , —, D. C. Welsh, and S. Y. Matrosov, 1992: Cloud layers, particle identification, and rain-rate profiles from ZRV_f measurements by clear-air Doppler radars. *J. Atmos. Oceanic Technol.*, **9**, 108–119.
- Hanczor, M., and M. Kumar, 1993: 12-kW S-band solid-state transmitter for modern radar systems. *IEEE Trans. Microwave Theory Tech.*, **41**, 2237–2243.
- Hartmann, D. L., H. H. Hendon, and R. A. Houze Jr., 1984: Some implications of the mesoscale circulations in tropical cloud clusters for large-scale dynamics and climate. *J. Atmos. Sci.*, **41**, 113–121.
- Houze, R. A., Jr., 1989: Observed structure of mesoscale convective systems and implications for large-scale heating. *Quart. J. Roy. Meteor. Soc.*, **115**, 425–461.
- Johnson, R. H., 1984: Partitioning tropical heat and moisture budgets into cumulus and mesoscale components: Implications for cumulus parameterization. *Mon. Wea. Rev.*, **112**, 1590–1601.
- Joss, J., and A. Waldvogel, 1990: Precipitation measurement and hydrology. *Radar in Meteorology*, D. Atlas, Ed., Amer. Meteor. Soc., 577–606.
- Keenan, T., R. Carbone, S. Rutledge, J. Wilson, G. Holland, and P. May, 1996: The Maritime Continent Thunderstorm Experiment (MCTEX): Overview and initial results. Preprints, *Seventh Conf. on Mesoscale Processes*, Reading, United Kingdom, Amer. Meteor. Soc., 326–328.
- Knight, C. A., and L. J. Miller, 1993: First radar echoes from cumulus clouds. *Bull. Amer. Meteor. Soc.*, **74**, 179–188.

- Lhermitte, R., 1987: A 94-GHz Doppler radar for cloud observations. *J. Atmos. Oceanic Technol.*, **4**, 36–48.
- Lubin, D., J.-P. Chen, P. Pilewski, V. Ramanathan, and F. P. J. Valero, 1996: Microphysical examination of excess cloud absorption in the tropical atmosphere. *J. Geophys. Res.*, **101**, 16 961–16 972.
- Matrosov, S. Y., 1992: Radar reflectivity in snowfall. *IEEE Trans. Geosci. Remote Sens.*, **30**, 454–461.
- Parsons, D., and Coauthors, 1994: The integrated sounding system: Description and preliminary observations from TOGA COARE. *Bull. Amer. Meteor. Soc.*, **75**, 553–567.
- Ralph, F. M., 1995: Using radar-measured radial vertical velocities to distinguish precipitation scattering from clear-air scattering. *J. Atmos. Oceanic Technol.*, **12**, 257–267.
- Rogers, R. R., and W. O. J. Brown, 1997: Radar observations of a major industrial fire. *Bull. Amer. Meteor. Soc.*, **78**, 803–814.
- , W. L. Ecklund, D. A. Carter, K. S. Gage, and S. A. Ethier, 1993a: Research applications of a boundary-layer wind profiler. *Bull. Amer. Meteor. Soc.*, **74**, 567–580.
- , D. Baumgardner, S. A. Ethier, D. A. Carter, and W. L. Ecklund, 1993b: Comparison of raindrop size distributions measured by radar wind profiler and by airplane. *J. Appl. Meteor.*, **32**, 694–699.
- Sassen, K., 1987: Ice cloud content from radar reflectivity. *J. Climate Appl. Meteor.*, **26**, 1050–1053.
- Sekelsky, S. M., and R. E. McIntosh, 1996: Cloud observations with a polarimetric 33-GHz and 95-GHz radar. *Meteor. Atmos. Phys.*, **59**, 123–140.
- , W. L. Ecklund, J. M. Firda, K. S. Gage, and R. E. McIntosh, 1999: Particle size estimation in ice-phase clouds using multi-frequency radar reflectivity measurements at 95, 33, and 2.8 GHz. *J. Appl. Meteor.*, **38**, 5–28.
- Wakasugi, K., S. Fukao, S. Kato, A. Mizutani, and M. Matsuo, 1985: Air and precipitation particle motions within a cold front measured by the MU VHF radar. *Radio Sci.*, **20**, 1233–1240.
- , B. B. Balsley, and T. L. Clark, 1987: The VHF Doppler radar as a tool for cloud and precipitation studies. *J. Atmos. Oceanic Technol.*, **4**, 273–280.
- Wilczak, J. M., and Coauthors, 1995: Contamination of wind profiler data by migrating birds: Characteristics of corrupted data and potential solutions. *J. Atmos. Oceanic Technol.*, **12**, 449–467.
- Williams, C. R., W. L. Ecklund, and K. S. Gage, 1995: Classification of precipitating clouds in the Tropics using 915-MHz wind profilers. *J. Atmos. Oceanic Technol.*, **12**, 996–1012.
- Wilson, J. W., T. M. Weckwerth, J. Vivekanandan, R. M. Wakimoto, and R. W. Russell, 1994: Boundary layer clear-air radar echoes: Origin of echoes and accuracy of derived winds. *J. Atmos. Oceanic Technol.*, **11**, 1184–1206.